American Journal of Analytical Chemistry, 2015, 6, 457-467
Published Online April 2015 in SciRes. http://www.scirp.org/journal/ajac
http://dx.doi.org/10.4236/ajac.2015.65045

Determination of ppt Level Chromium(VI) Using the Gold Nano-Flakes Electrodeposited on Platinum Rotating Disk Electrode and Modified with 4-Thiopyridinium

Huy Du Nguyen[1], T. Thuy Luyen Nguyen[1], Khac Manh Nguyen[1], T. Anh Tuyet Tran[1], Anh Mai Nguyen[1], Quoc Hien Nguyen[2*]

[1]Central Laboratory for Analysis, University of Science, Vietnam National University in Ho Chi Minh City, Ho Chi Minh City, Vietnam
[2]Research and Development Center for Radiation Technology, Vietnam Atomic Energy Institute, Ho Chi Minh City, Vietnam
Email: *hien7240238@yahoo.com

Received 13 March 2015; accepted 13 April 2015; published 17 April 2015

Abstract

The nano-gold layer formed on the platinum rotating disk electrode (nano-Au/Pt-RD) inherited the catalytic property for Cr(VI) reduction from platinum surface and owned the good features of nano-gold such as insensitivity with hydrogen ion, high surface area, augmenting diffusion of Cr(VI) and ability for self-assembling with 4-pyridine-ethanethiol (PET) through Au←S linkages, to form PET/nano-Au/Pt-RD electrode capable of accumulating Cr(VI) from sample. The obtained PET/nano-Au/Pt-RD electrode showed an extreme sensitivity to Cr(VI). By using this electrode, 1.09 ng·L^{-1} was the detection limit of differential pulse adsorptive cathodic stripping voltammetry for Cr(VI) with the accumulation time of only 2 min. Moreover, this electrode was reproducible with 3.5% RSD for 30 times of Cr(VI) accumulating and stripping. In addition, this electrode was also selective for Cr(VI) determination, which was not almost interfered by other inorganic ions.

Keywords

Nano-Gold Layer, Platinum Electrode, Stripping Voltammetry

---

[*] Corresponding author.

How to cite this paper: Nguyen, H.D., Nguyen, T.T.L., Nguyen, K.M., Tran, T.A.T., Nguyen, A.M. and Nguyen, Q.H. (2015) Determination of ppt Level Chromium(VI) Using the Gold Nano-Flakes Electrodeposited on Platinum Rotating Disk Electrode and Modified with 4-Thiopyridinium. *American Journal of Analytical Chemistry*, **6**, 457-467.
http://dx.doi.org/10.4236/ajac.2015.65045

1. Introduction

Hexavalent chromium (Cr(VI)) is a strong oxidizing and toxic agent [1]-[9]. Cr(VI) is also recognized as an animal and human carcinogen [1]-[5]. The development of analytical method for Cr(VI) at trace level is a matter of great interest in analytical chemistry [2]-[9]. Electrochemical methods have been suitable ones for the Cr(VI) determination, because these methods possessed good selectivity and sensitivity [2]-[6]. A well-known electrochemical technique for the Cr(VI) determination is voltammetry using mercury electrodes [10] [11] or bismuth film electrodes [12]-[15]. Although extremely sensitive, these applications are limited because of potential toxicity of mercury and bismuth [3] [4]. In the effort to replace the toxic electrode, noble-metal electrodes including Pt, Au, etc. have been studied. A poly(4-vinylpryidinium)-coated platinum electrode was studied for preconcentration of Cr(VI) into the polymer films followed by voltammetric determination without interference by metal cations such as Cr^{3+} [16]-[18]. While highly sensitive, the coating of poly(4-vinylpryidinium) on platinum electrode is quite complex. Self-assembled monolayer of pyridinium [19] or azacrown [20] on the gold electrode has been also developed for attraction of Cr(VI) into the electrode before electrochemical detection. Through Au←S linkages, the coating of organic ligands on gold electrode is quite favorable.

However, the major drawback of gold-based electrodes is to require complex electrochemical and mechanical pretreatments to achieve reproducibility [21] [22]. According to Dai *et al*. [23], the renewal of the gold film before each measurement improved the reproducibility.

Several recent works have been based on the layer of gold nanoparticles for improvement of electrochemical detection of Cr(VI) for instance gold nanoparticle-modified glassy carbon electrode by electrodeposition [24] or gold nanoparticle-modified titania nanotubes electrode by photo-deposition [25]. Moreover, Ouyang *et al*. used 4-pyridine-ethanethiol (PET) to functionalize the gold nanoparticles on a glassy carbon electrode for accumulation of Cr(VI) in fluoride buffer (pH 4.5) before voltammetric determination by cathodic stripping square wave voltammetry [3]. Although fabrication procedure of working electrode was complex and time-consuming (24 h), Ouyang *et al*. [3] obtained the detection limit of 150 $ng \cdot L^{-1}$ that was 120-fold higher than that obtained by Turyan and Mandler [19] when using a gold-based electrode functionalized with PET and a same time for accumulation of Cr(VI).

Therefore, fabrication of nano-gold layer for Cr(VI) detection is necessary to study further. In this paper, gold nano-flakes are electrodeposited on platinum rotating disk electrode (Pt-RDE) directly to form nano-Au/Pt-RD electrode, then the resulting electrode is self-assembled with PET molecules through Au←S linkages to obtain PET/nano-Au/Pt-RD electrode using as working electrode for voltammetric determination of Cr(VI). By a suitable electrodeposition, the obtained gold nano-flakes are able to possess the advantages of both platinum surface and gold nanoparticle. The gold nano-flakes are selected to prevent Cr(VI) from reaction with small gold nanoparticles, because the antioxidant efficiency of gold nanoparticles decreased with the increase of their size [26].

2. Experimental

2.1. Chemical and Reagents

$HAuCl_4 \cdot 3H_2O$, $K_2Cr_2O_7$, NaF, HF, NaOH, HCl, H_2SO_4 and ethanol were of PA-grade and purchased from Merck (Germany). 4-Pyridine-ethanethiol hydrochloride (PET) was of PA-grade and purchased from Sigma-Aldrich (Singapore). Deionized water (purified by Mili-Q, Millipore, France) was used throughout all experiments. Stock standard solutions of Cr(VI) (*ca.* 1000 $mg \cdot L^{-1}$) were prepared in water and stored at 4˚C in a week. Working standard solutions were prepared in NaF buffer solutions and used in each experiment. NaF buffer solutions were prepared by dissolving 6.30 g of NaF in 1000 mL of water (*ca*. 0.15 M NaF) and adjusted pH to 4.5 or 7.8, respectively by adding 0.2 M HF solution or 0.2 M NaOH solution. Gold(III) solution was prepared from $HAuCl_4 \cdot 3H_2O$ in the solution of 0.5 M H_2SO_4. 30 mM PET solution was prepared from PET in the solution of 0.1 M H_2SO_4.

2.2. Apparatus

All electrochemical experiments and measurements were carried out on a Metrohm 757 VA Computrace potentiostat consisting of a typical three-electrode cell (Metrohm Ltd., Switzerland). The cell contains an Ag/AgCl (3 M KCl) reference electrode, the platinum wire counter electrode and a platinum (Pt) or glassy carbon (GC) rotating disk (RD) working electrode with disk diameter of 2 mm.

2.3. Working Electrode Preparations

2.3.1. Gold Nano-Flake Deposition

The nano-gold layer on platinum rotating disk electrode (nano-Au/Pt-RDE) is prepared by the potentiostat operating in DC mode and the typical three-electrode cell. The Pt-RDE was polished with the water slurry of 0.05 µm alumina particles. The residual polishing material was removed using ethanol and then water in an ultrasonic bath. After conditioning in 0.25 M H_2SO_4 solution at 400 mV for 10 min, the Pt-RDE was immersed into 3 mM $HAuCl_4$ solution and rotated at 400 rpm. Deposition was conducted at the applied potential of −200 mV (*vs.* Ag/AgCl, 3 M KCl) for 3 min. Finally, the nano-Au/Pt-RDE was washed with water and the surface of working electrode was activated in 0.15 M NaF buffer solution pH 7.8 by the linear potential sweep with potential range from 400 to −200 mV and scan rate of 10 $mV \cdot s^{-1}$ until the voltammetric response was reproducible.

2.3.2. PET Modification

The nano-Au/Pt-RDE was rotated at 600 rpm into the 30 mM PET solution for 10 min. The PET-modified nano-Au/RDE (PET/nano-Au/Pt-RDE) were conditioned in 0.1 M $HClO_4$ solution by electrocycling with potential range from 400 to −200 mV and scan rate of 10 $mV \cdot s^{-1}$ until the voltammetric response was reproducible.

2.4. Electrode Characterization

The surface of working electrode was firstly activated in a 0.15 M NaF buffer solution pH 7.8 by the linear potential sweep with potential range from 400 to −100 mV and scan rate of 5 $mV \cdot s^{-1}$. After obtaining reproducible voltammograms, 100 $mg \cdot L^{-1}$ Cr(VI) was added into the cell to evaluate the activity of the obtained electrode for the Cr(VI) reduction.

The surface morphology of the nano gold layers was examined by a field emission scanning electron microscope-FESEM-(Hitachi, S-4800, Japan). The nano-Au layer was taken out of the surface of Pt-RDE by adhesive carbon tape before SEM photograph.

2.5. Cr(VI) Analysis

2.5.1. Measurement Procedure

The PET/nano-Au/Pt-RDE was first put in 10 mL of sample or sample spiked Cr(VI) pH 4.5 consisting of 0.15 M NaF and rotated at 400 rpm under open-circuit potential to accumulate Cr(VI) for 2 min. After the accumulation, the determination of Cr(VI) was carried out by transferring the electrodes to 0.15 M NaF buffer solution pH 7.8 without Cr(VI) and performing differential pulse adsorptive cathodic stripping voltammetry (DPAdCSV) from 400 to −100 mV with scan rate of 50 $mV \cdot s^{-1}$ (potential step of 5 mV and time step of 0.1 s) and amplitude of 50 mV under non-stirring. The electrode surface was regenerated between measurements by electrocycling in 0.1 M $HClO_4$ for eliminating Cr(VI) from the electrode surface.

2.5.2. Sample Preparation

Coastal water sample was filtered by 0.45 µm membrane filter and diluted at least 5000 times by 0.15 M NaF buffer solution pH 4.5.

3. Results and Discussion

3.1. The Nano-Au/Pt-RD Electrode

3.1.1. Electrodeposition

The electrodeposition of gold nano-flakes (nano-Au) on platinum surface from $HAuCl_4$ solution depends on the $HAuCl_4$ concentration($C_{Au(III)}$), the rotating speed of electrode (V_R), the deposition potential (E_P), the deposition time (t_P) and temperature (T_P). Therefore, $C_{Au(III)}$, V_R, E_P and t_P were investigated while the T_P was kept constant at 25˚C.

The activity of the nano-Au/Pt-RDE deposited was evaluated by the peak current (I_P) obtained when electrode potential was swept from 400 to −100 mV with scan rate of 5 $mV \cdot s^{-1}$ in 0.15 M NaF buffer solution pH 7.8 consisting of 100 $mg \cdot L^{-1}$ Cr(VI). Each electrodeposition condition of nano-Au was repeated three times to evaluate the reproducibility of electrodeposition through standard deviation (SD) of I_P.

The E_P conducted the activity of the Pt-RDE for the reduction of $HAuCl_4$ into nano-Au. The highest I_P was obtained with E_P of −200 mV (**Figure 1**). When E_P was more negative, the reduction of hydrogen ion affected the deposition of the nano-Au, which caused rapid diminution of I_P.

The V_R governed the transferring rate of $HAuCl_4$ to electrode surface. Thus, the thickness of deposited layer increased with V_R. Increasing the thickness made nano-Au layer rougher and the electrochemically active surface of the obtained nano-Au/Pt-RDE larger [27]. Consequently, the I_P increased. The highest I_P was obtained with V_R of 400 rpm (**Figure 2**). When the thickness was too high, nano-Au layer could lose the catalytic property inheriting from platinum surface [28], which caused rapid diminution of I_P.

The thickness of nano-gold layer increased with the increase of $C_{Au(III)}$ and t_P. **Figure 3** and **Figure 4** showed that the SD values of I_P rapidly increased at high values of the $C_{Au(III)}$ and t_P. This might be ascribed to the rapid changing from platinum to gold property when the thickness of nano-Au layer was high enough. **Figure 3** indicated that an optimal $C_{Au(III)}$ was 3 mM. Similarly, an optimal t_P was 3 min (**Figure 4**).

3.1.2. Activity and Morphology

Figure 5 depicts the voltammetric responses of Au-RDE (a), nano-Au/GC-RDE (b), nano-Au/Pt-RDE (c) and Pt-RDE (d) obtained for 100 mg·L^{-1} Cr(VI) in 0.15 M NaF buffer pH 7.8. The NaF buffer is used as electrolyte because it is suitable for all of the electrodes studied [3] [16]-[19]. The Au-RDE showed the lowest peak current while the Pt-RDE exhibited the highest peak current for Cr(VI) reduction. However, the Pt-RDE also gave a high wave of hydrogen ion reduction near the wave of Cr(VI) reduction. The hydrogen wave could interfere to Cr(VI) determination at trace level.

The peak current of the nano-Au/GC-RDE is greatly higher than that of the Au-RDE. This phenomenon was also observed in the study of Chen *et al*. [25]. The considerable enhancement of the peak current was usually attributed to the high surface area of the nano-Au layer [25] [29] and the advantageous diffusion of Cr(VI) to the nano-Au layer [25] [30] because the surface of the nano-Au/GC-RDE is rougher than the surface of Au-RDE (**Figure 6(A)**). In addition, the peak potential for Cr(VI) reduction on the nano-Au/GC-RDE was found at 80 mV, approximating to the potential observed on the gold nanoparticle-modified electrode of the previous studies [3] [25].

It is interesting that the peak potential for Cr(VI) reduction on the nano-Au/Pt-RDE and the Pt-RDE was found at 160 mV and it was 80 mV more positive than that of the nano-Au/GC-RDE. The positive shifting of Cr(VI) reductive potential showed that Cr(VI) reduction on the nano-Au/Pt-RDE and the Pt-RDE was easier than that on the nano-Au/GC-RDE. On the other hand, the peak current of the nano-Au/Pt-RDE was significantly higher than the one of the nano-Au/GC-RDE while the surface of the nano-Au/Pt-RDE (**Figure 6(B)**) was less rugged than the nano-Au/GC-RDE (**Figure 6(A)**). Therefore, the activity for Cr(VI) reduction of the nano-Au/Pt-RDE was higher than the activity of the nano-Au/GC-RDE.

The peak current of the nano-Au/Pt-RDE was similar to the one of the Pt-RDE while the hydrogen wave did not appear on the nano-Au/Pt-RDE. This indicated that the nano-Au layer on the nano-Au/Pt-RDE covered nearly whole of platinum surface of Pt-RDE and copied the catalysis of platinum surface for Cr(VI) reduction. Thus, the nano-Au/Pt-RDE possessed the catalysis of platinum surface and the advantages of gold nanoparticle such as insensitiveness with hydrogen ion and convenience for assembling with PET to accumulate Cr(VI). Therefore, the nano-Au/Pt-RDE was better than Pt-RDE and nano-Au/GC-RDE.

3.2. The PET/Nano-Au/Pt-RD Electrode

3.2.1. PET Assembling

According to Ouyang *et al*. [3], the more the number of the pyridium groups on working electrode were, the more quickly and thoroughly the accumulation of Cr(VI) took place. The nano-Au/Pt-RDE possessed a higher surface area than the Au-RDE did. Thus, the PET concentration used was 30 mM, which was 6-fold higher than that of the previously published reports [3] [19]. For optimizing nano-Au layer assembling with the PET molecules, immersion time of electrode (t_I) in PET solution was surveyed with the PET concentration of 30 mM and the electrode rotation speed of 600 rpm. The quality of the PET/nano-Au/Pt-RDE was evaluated by the amount of Cr(VI) was accumulated into the obtained electrode from 0.15 NaF buffer solution pH 4.5 consisting of 10 ng·L^{-1} Cr(VI). The amount of Cr(VI) accumulated gave the Cr(VI) reductive current peak when the electrode potential was swept from 400 mV to –100 mV in NaF buffer pH 7.8 by DPAdCSV. **Figure 7** showed that the optimum of t_I was 10 min.

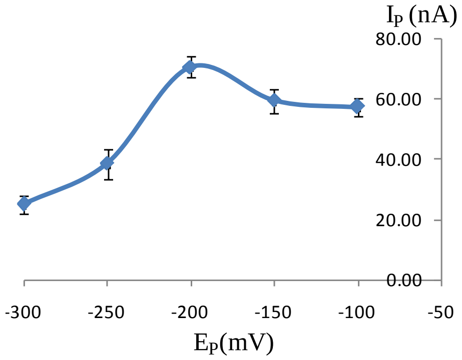

Figure 1. The reductive peak current (I_P) of 100 mg·L^{-1} Cr(VI) on the obtained nano-Au/Pt-RDE as a function of deposition potential used for electrodeposition of this electrode.

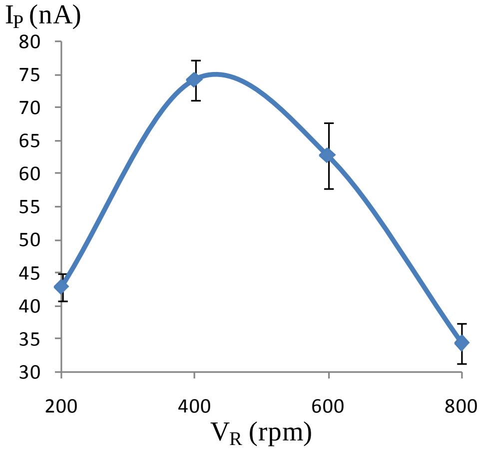

Figure 2. The reductive peak current (I_P) of 100 mg·L^{-1} Cr(VI) on the obtained nano-Au/Pt-RDE as a function of rotating rate used for electrodeposition of this electrode.

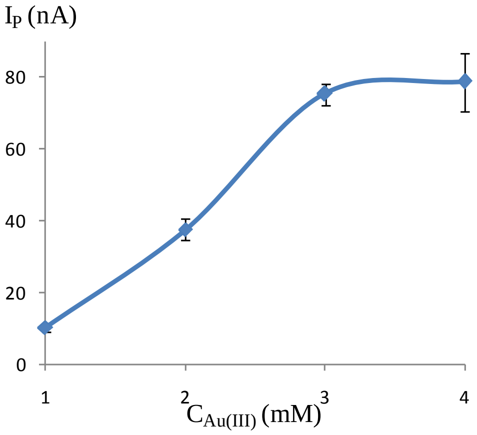

Figure 3. The reductive peak current (I_P) of 100 mg·L^{-1} Cr(VI) on the obtained nano-Au/Pt-RDE as a function of $HAuCl_4$ concentration used for electrodeposition of this electrode.

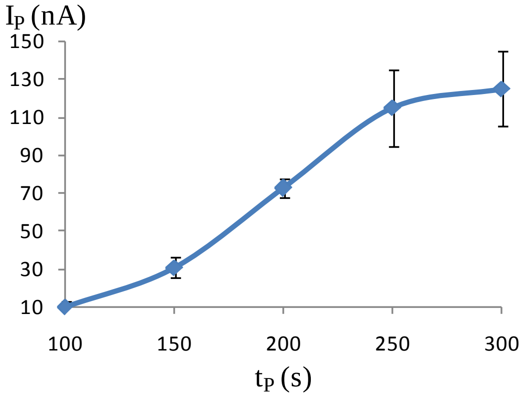

Figure 4. The reductive peak current (I_P) of 100 mg·L^{-1} Cr(VI) on the obtained nano-Au/Pt-RDE as a function of deposition time used for electrodeposition of this electrode.

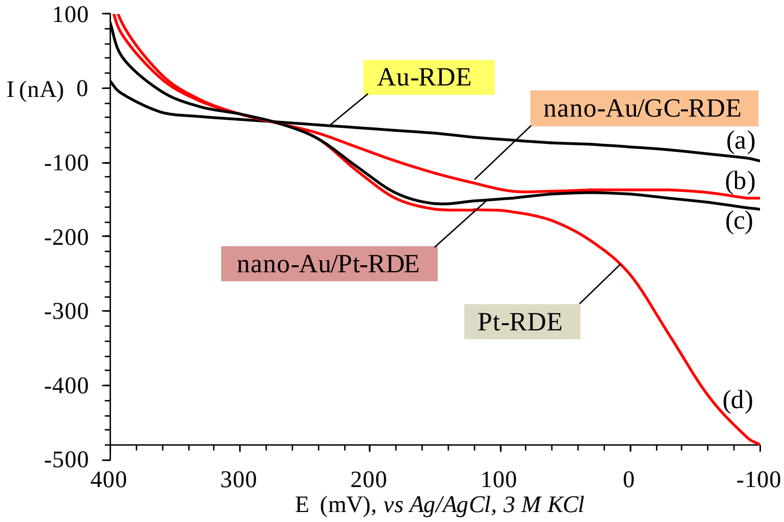

Figure 5. Voltammetric response of Au-RDE (a), nano-Au/GC-RDE (b), nano-Au/Pt-RDE (c) and Pt-RDE (d) toward 100 mg·L^{-1} Cr(VI) in 0.15 M NaF buffer (pH 7.8) when potential was linearly swept from 400 to –100 mV with scan rate of 5 mV·s^{-1}.

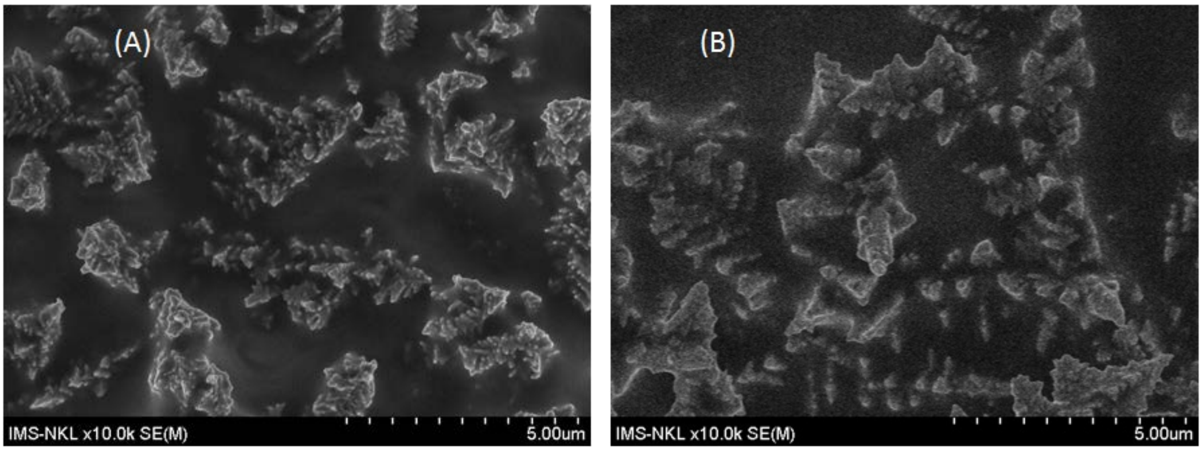

Figure 6. The SEM micrograph of the nano-Au/GC-RDE (A) and the nano-Au/Pt-RDE (B).

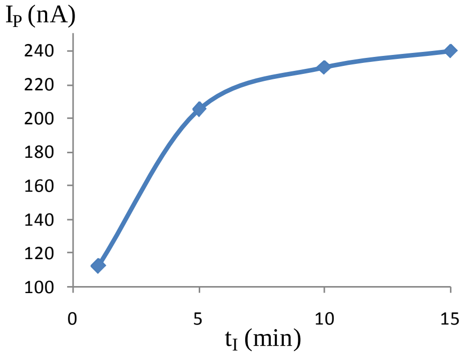

Figure 7. The reductive peak current (I_P) of Cr(VI) accumulated on the obtained PET/nano-Au/Pt-RDE as a function of immersion time used for PET assembling of this electrode.

3.2.2. Behavior of Electrode

For direct electroreduction of Cr(VI) in 0.15 M NaF buffer pH 7.8, the PET/nano-Au/Pt-RDE showed the peak current that is 30% lower than that of the nano-Au/Pt-RDE. This result indicated that the PET molecules have been assembled on the nano-Au/Pt-RDE and they could make the electrochemically active surface of the PET/nano-Au/Pt-RDR smaller than the surface of nano-Au/Pt-RDE.

Figure 8(A) showed the differential pulse adsorptive cathodic stripping voltammogram of the PET/nano-Au/Pt-RDE in 0.15 M NaF buffer pH 7.8 after preconcentrating Cr(VI) from 0.15 M NaF buffer pH 4.5 consisting of Cr(VI) in the concentration range from 2.5 to 40 ng·L^{-1}. The PET/nano-Au/Pt-RDE showed well-defined peaks at ~240 mV vs Ag/AgCl, 3 M KCl and the peak current proportionally increased with the concentration of Cr(VI) in the NaF buffer pH 4.5. Thus, this peak was attributed to the electrochemical reduction of Cr(VI) to Cr(III). This indicated that the PET/nano-Au/Pt-RDE was able to preconcentrate Cr(VI) from the NaF buffer pH 4.5 into it.

Using the accumulation time of 2 min, the linear response for Cr(VI) was observed over the concentration range from 2.5 to 40 ng·L^{-1} with a correlation coefficient of 0.999 (**Figure 8(B)**) when the peak current was used as a function of the Cr(VI) concentration in the NaF buffer pH 4.5. The detection limit was of 1.09 ppt based on three times the standard deviation of the baseline [24]. Although the accumulation time was shorter, the PET/nano-Au/Pt-RDE still showed the LOD lower than the LOD of previous studies [2]-[6] [10]-[20].

The reproducibility of the PET/nano-Au/Pt-RDE was estimated from the DPAdCSV peak current of 25 ng·L^{-1} Cr(VI) in NaF buffer solution pH 4.5. Results in **Figure 9** showed that the peak currents were in the range from 95% to 105% of the average value with relative standard deviation (RSD) of 3.4% when the accumulating and stripping Cr(VI) were repeated 30 times on the same PET/nano-Au/Pt-RDE. This reproducibility showed that the PET/nano-Au/Pt-RDE is suitable for standard addition method.

Beside good sensitivity and reproducibility, the PET/nano-Au/Pt-RDE also showed a high selectivity for the accumulating and stripping Cr(VI). The NaF buffer solutions (pH 4.5) consisting of 20 ng·L^{-1} Cr(VI) and 20 mg·L^{-1} investigated ions exhibited the DPAdCSV peak currents which were in the range from 95% to 105% of the peak current of the NaF buffer solution (pH 4.5) consisting of 20 ng·L^{-1} Cr(VI) (**Figure 10**). Therefore, the ions such as Cr^{3+}, Fe^{3+}, Cu^{2+}, Mg^{2+}, Ca^{2+}, K^+, Na^+, SO_4^{2-}, ClO_4^-, NO_3^- and Cl^- could not interfere to DPAdCSV of Cr(VI) on PET/nano-Au/Pt-RDE even though their contents were million-fold higher than that of Cr(VI).

The analytical reliability and potential practical applications of new electrode (PET/nano-Au/Pt-RDE) were confirmed by measuring Cr(VI) in real samples. Coastal water samples containing low content of Cr(VI) and high content of other ions are suitable to evaluate the performance of new electrode. After eliminating suspended impurities, the coastal water samples were diluted 5000 times by 0.15 M NaF buffer pH 4.5. The data of Cr(VI) analysis on the PET/nano-Au/Pt-RDE was shown in **Figure 11**. The slope of the standard addition curve of Cr(VI) on the coastal water sample (**Figure 11(B)**) was very close to the slope of the standard curve of Cr(VI) (**Figure 8(B)**). This showed that the sample background did not interfere to Cr(VI) determination on the PET/nano-Au/Pt-RDE. The relative standard deviation (RSD) of the result was of 6.24%.

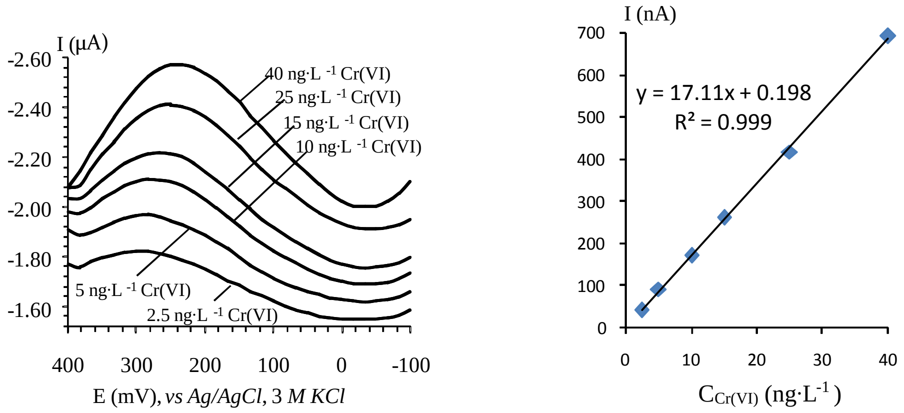

(A) (B)

Figure 8. DPAdCS voltammograms of PET/nano-Au/Pt-RDE in 0.15 M NaF buffer pH 7.8 toward the reduction of Cr(VI) adsorbed from 0.15 M NaF buffer pH 4.5 consisting of Cr(VI) in the concentration range from 2.5 to 40 ng·L^{-1} (A) and corresponding calibration plot (B).

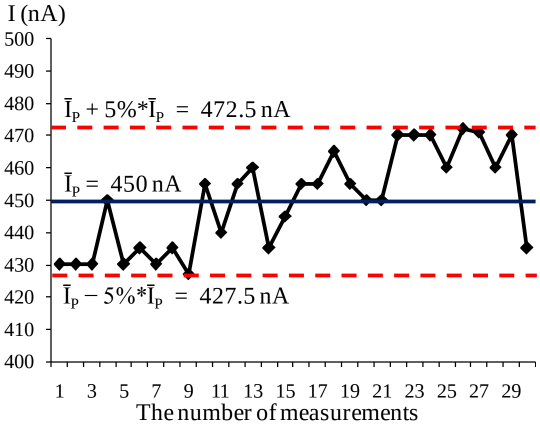

Figure 9. The reproducibility of the DPAdCSV peak current of the PET/nano-Au/Pt-RDE in 0.15 M NaF buffer pH 7.8 toward the reduction of Cr(VI) adsorbed from 0.15 M NaF buffer pH 4.5 consisting of 25 ng·L^{-1} Cr(VI).

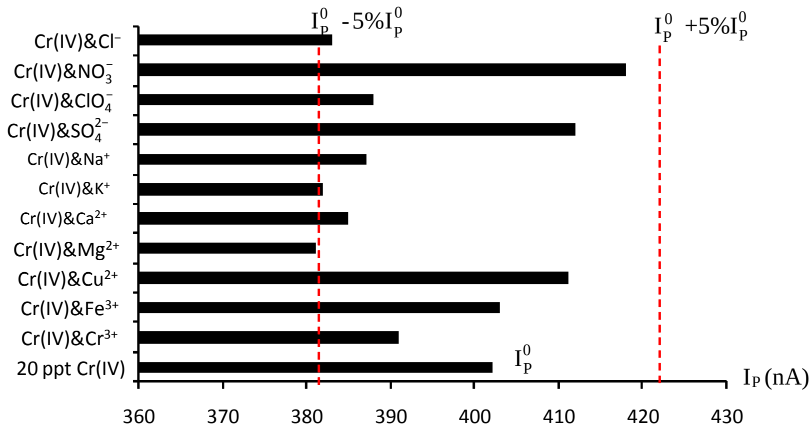

Figure 10. The DPAdCSV peak current of the PET/nano-Au/Pt-RDE in 0.15 M NaF buffer pH 7.8 toward the reduction of Cr(VI) adsorbed from 0.15 M NaF buffer (pH 4.5) consisting of 20 ng·L^{-1} Cr(VI) or 20 ng·L^{-1} Cr(VI) and 20 mg·L^{-1} another ion such as: Cr^{3+}, Fe^{3+}, Cu^{2+}, Mg^{2+}, Ca^{2+}, K^+, Na^+, SO_4^{2-}, ClO_4^-, NO_3^-, and Cl^-.

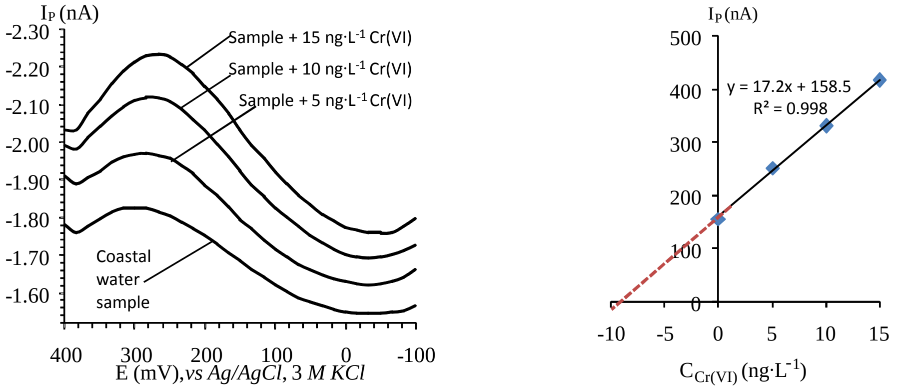

(A) (B)

Figure 11. DPAdCS voltammograms of PET/nano-Au/Pt-RDE in 0.15 M NaF buffer pH 7.8 toward the reduction of Cr(VI) adsorbed from diluted sample pH 4.5 consisted of 0.15 M NaF and diluted samples spiked Cr(VI) (A) and corresponding standard addition plot (B).

4. Conclusion

Electrodeposition approach is incomplex, time-saving and reproducible. Through this study, the PET/nano-Au/Pt-RDE was successfully fabricated by a simple electrodeposition method. This new electrode likely enhances the sensitivity and reproducibility of the DPAdCSV method for determining Cr(VI). With the accumulation time of about 2 min, the low LOD (1 ppt) and LOQ (2.5 ppt) showed that the nano-Au layer possesses the new electrochemical property. The obtained results indicated that the nano-Au layer formed on the platinum rotating disk electrode (nano-Au/Pt-RDE) inherited the catalytic property for Cr(VI) reduction from platinum surface and owned the good features of gold nanoparticles such as insensitivity with hydrogen ion, high surface area, augmented diffusion of Cr(VI) and ability for self-assembling with 4-pyridine-ethanethiol (PET) through Au←S linkages.

Acknowledgements

This research is funded by Vietnam National University HoChiMinh City (VNU-HCM) under grant number B2012-18-30.

References

[1] Odeh, L., Odeh, I., Khamis, M., Khatib, M., Qurie, M., Shakhsher, Z. and Qutob, M. (2015) Hexavalent Chromium Removal and Reduction to Cr(III) by Polystyrene Tris(2-aminoethyl)-amine. *American Journal of Analytical Chemistry*, **6**, 26-37. http://dx.doi.org/10.4236/ajac.2015.61003

[2] Kachoosangi, R.T. and Compton, R.G. (2013) Voltammetric Determination of Chromium(VI) Using a Gold Film Modified Carboncomposite Electrode. *Sensor and Actuators B*, **178**, 555-562. http://dx.doi.org/10.1016/j.snb.2012.12.122

[3] Ouyang, R., Bragg, S.A., Chambers J.Q. and Xue, Z.L. (2012) Flower-Like Self-Assembly of Gold Nanoparticles for Highly Sensitive Electrochemical Detection of Chromium(VI). *Analytica Chimica Acta*, **722**, 1-7. http://dx.doi.org/10.1016/j.aca.2012.01.032

[4] Jena, B.K. and Raj, C.R. (2008) Highly Sensitive and Selective Electrochemical Detection of Sub-ppb Level Chromium(VI) Using Nano-Sized Gold Particle. *Talanta*, **76**,161-165. http://dx.doi.org/10.1016/j.talanta.2008.02.027

[5] Xu, H., Zheng, Q., Yang, P., Liu, J., Xing, S. and Jin, L.(2011) Electrochemical Synthesis of Silver Nanoparticles-Coated Gold Nanoporous Film Electrode and Its Application to Amperometric Detection for Trace Cr(VI). *Science China Chemistry*, **54**, 1004-1010. http://dx.doi.org/10.1007/s11426-011-4261-7

[6] Cox, J.A., West, J.L. and Kulesza, P.J. (1984) Determination of Chromium(V1) by Differential-Pulse Polarography with a Sodium Fluoride Supporting Electrolyte. *Analyst*, **109**, 927-930. http://dx.doi.org/10.1039/an9840900927

[7] Idriss, K.A., Sedaira, H. and Dardeery, S. (2013) Spectrophotometric Determination of Water-Soluble Hexavalent Chromium and Determination of Total Hexavalent Chromium Content of Portland Cement in the Presence of Iron(III) and Titanium(IV) Using Derivative Ratio Spectrophotometry. *American Journal of Analytical Chemistry*, **4**, 653-660.

http://dx.doi.org/10.4236/ajac.2013.411078

[8] Cesph-Romero, R.M., Yebra-Biurrun, M.C. and Bermejo-Barrera, M.P. (1996) Preconcentration and Speciation of Chromium by the Determination of Total Chromium and Chromium(III) in Natural Waters by Flame Atomic Absorption Spectrometry with a Chelating Ion-Exchange Flow Injection System. *Analytica Chimica Acta*, **327**, 37-45. http://dx.doi.org/10.1016/0003-2670(96)00062-1

[9] Pantsar-Kallio, M. and Manninen, P.K.G. (1996) Speciation of Chromium in Aquatic Samples by Coupled Column Ion Chromatography-Inductively Coupled Plasma-Mass Spectrometry. *Analytica Chimica Acta*, **318**, 335-343. http://dx.doi.org/10.1016/0003-2670(95)00448-3

[10] Crosmun, S.T. and Mueller, T.I. (1975) The Determination of Chromium(VI) in Natural Waters by Differential Pulse Polarography. *Analytica Chimica Acta*, **75**, 199-205. http://dx.doi.org/10.1016/S0003-2670(01)81967-X

[11] Boussemart, M., van den Berg, C.M.G. and Ghaddaf, M. (1992) The Determination of the Chromium Speciation in Sea Water Using Catalytic Cathodic Stripping Voltammetry. *Analytica Chimica Acta*, **262**, 103-115. http://dx.doi.org/10.1016/0003-2670(92)80014-X

[12] Wang, J., Lu, J., Hocevar, S.B., Farias, P.A.M. and Ogorevc, B. (2000) Bismuth-Coated Carbon Electrodes for Anodic Stripping Voltammetry. *Analytical Chemistry*, **72**, 3218-3222. http://dx.doi.org/10.1021/ac000108x

[13] Wang, J., Lu, J., Kirgöz, Ü.A., Hocevar, S.B. and Ogorevc, B. (2001) Insights into the Anodic Stripping Voltammetric Behavior of Bismuth Film Electrodes. *Analytica Chimica Acta*, **434**, 29-34. http://dx.doi.org/10.1016/S0003-2670(01)00818-2

[14] Lin, L., Lawrence, N.S., Thongngamdee, S., Wang, J. and Lin, Y. (2005) Catalytic Adsorptive Stripping Determination of Trace Chromium (VI) at the Bismuth Film Electrode. *Talanta*, **65**, 144-148. http://dx.doi.org/10.1016/j.talanta.2004.05.044

[15] Ouyang, R., Zhang, W., Zhou, S., Xue, Z.-L., Xu, L., Gu, Y. and Miao, Y. (2013) Improved Bi Film Wrapped Single Walled Carbon Nanotubes for Ultrasensitive Electrochemical Detection of Trace Cr(VI). *Electrochimica Acta*, **113**, 686-693. http://dx.doi.org/10.1016/j.electacta.2013.09.110

[16] Cox, J.A. and Kulesza, P.J. (1983) Stripping Voltammetry of Chromium(VI) at a Poly(4-Vinylpyri-Dine)-Coated Platinum Electrode. *Analytica Chimica Acta*, **154**, 71-78. http://dx.doi.org/10.1016/0003-2670(83)80007-5

[17] Cox, J.A. and Kulesza, P.J. (1983) Preconcentration and Voltammetric Behavior of Chromium(VI) at Pt Electrodes Modified with Poly(4-Vinylpyridine). *Journal of Electroanalytical Chemistry*, **159**, 337-346. http://dx.doi.org/10.1016/S0022-0728(83)80632-9

[18] Teasdale, P.R., Spencer, M.J. and Wallace, G.G. (1989) Selective Determination of Cr(VI) Oxyan-Ions Using a Poly-3-Methylthiophene-Modified Electrode. *Electroanalysis*, **1**, 541-547. http://dx.doi.org/10.1002/elan.1140010611

[19] Turyan, I. and Mandler, D. (1997) Selective Determination of Cr(VI) by a Self-Assembled Monolayer-Based Electrode. *Analytical Chemistry*, **69**, 894-897. http://dx.doi.org/10.1021/ac9607525

[20] Wei, J., Guo, Z., Chen, X., Han, D.-D., Wang, X.-K. and Huang, X.-J. (2015) Ultrasensitive and Ultraselective Impedimetric Detection of Cr(VI) Using Crown Ethers as High-Affinity Targeting Receptors. *Analytical Chemistry*, **87**, 1991-1998. http://dx.doi.org/10.1021/ac504449v

[21] Welch, C., Nekrassova, O., Dai, X., Hyde, M. and Compton, R.G. (2004) Fabrication, Characterisation and Voltammetric Studies of Gold Amalgam Nanoparticle Modified Electrodes. *ChemPhysChem*, **5**, 1405-1410. http://dx.doi.org/10.1002/cphc.200400263

[22] Okcu, F., Ertas, F.N., Gokcel, H.I. and Tural, H. (2005) Anodic Stripping Voltammetric Behavior of Mercury in Chloride Medium and Its Determination at a Gold Film Electrode. *Turkish Journal of Chemistry*, **29**, 355-366.

[23] Dai, X., Nekrassova, O., Hyde, M.E. and Compton, R.G. (2004) Anodic Stripping Voltammetry of Arsenic(III) Using Gold Nanoparticle-Modified Electrodes. *Analytical Chemistry*, **76**, 5924-5929. http://dx.doi.org/10.1021/ac049232x

[24] Liu, B.Z., Lu, L.Y., Wang, M. and Zi, Y.Q. (2008) A Study of Nanostructured Gold Modified Glassy Carbon Electrode for the Determination of Trace Cr(VI). *Journal Chemical Sciences*, **120**, 493-498. http://dx.doi.org/10.1007/s12039-008-0077-1

[25] Jin, W., Wu, G.S. and Chen, A.C. (2014) Sensitive and Selective Electrochemical Detection of Chromium(VI) Based on Gold Nanoparticle-Decorated Titania Nanotube Arrays. *Analyst*, **139**, 235-241. http://dx.doi.org/10.1039/C3AN01614E

[26] Nguyen, N.D., Dang, V.P., Le, A.Q. and Nguyen, Q.H. (2014) Electron Beam/γ-Ray Irradiation Synthesis of Gold Nanoparticles and Investigation of Antioxidant Activity. *Advances in Natural Sciences*: *Nanoscience and Nanotechnology*, **5**, Article ID: 045002. http://dx.doi.org/10.1088/2043-6262/5/4/045002

[27] Watanabe, T. (2004) Microstructure Control Theory of Plated Film. In: Watanabe, T., Ed., *Nano-Plating Microstructure Control Theory of Plated Film and Data Base of Plated Film Microstructure*, Elsevier, New York, 3-91. http://dx.doi.org/10.1016/B978-008044375-1/50010-5

[28] Lovric, M. (2010) Stripping Voltammetry. In: Scholz, F., Ed., Electroanalytical Methods Guide to Experiments and Applications, Springer, New York, 201-221. http://dx.doi.org/10.1007/978-3-642-02915-8_10

[29] Deng, L., Wang, Y.Z., Shang, L., Wen, D., Wang, F.A. and Dong, S.J. (2008) A Sensitive NADH and Glucose Biosensor Tuned by Visible Light Based on Thionine Bridged Carbon Nanotubes and Gold Nanoparticles Multilayer. *Biosensors and Bioelectronics*, **24**, 951-957. http://dx.doi.org/10.1016/j.bios.2008.07.066

[30] Oyama, M. (2010) Recent Nanoarchitectures in Metal Nanoparticle-Modified Electrodes for Electroanalysis. *Analytical Science*, **26**, 1-12. http://dx.doi.org/10.2116/analsci.26.1